Tailoring the surface of polymeric nanofibres generated by pressurised gyration spinning

U.E.Illangakoon[1], S. Mahalingam[1] , Paolo Colombo[2] , M. Edirisinghe[*1]

[1] Department of Mechanical Engineering, University College London, London WC1E 7JE, UK

[2] Dipartimento di Ingegneria Industriale, Università di Padova via Marzolo, 9 35131 Padova, Italy

Abstract

Polymeric nanofibers with smooth, rough and porous surfaces were prepared by using pressurized gyration which is a novel method to produce nanofibers, utilizing the combination of centrifugal spinning and solution blowing. Series of fibers were prepared by using Polyacrylonitrile (PAN),Poly(methyl methacrylate)(PMMA) and 50:50 PAN-PMMA polymer solutions without pressure and 0.2 MPa working pressure. The surface morphology of the nanofibers were analysed using scanning electron microscopy and thermal properties were studied using thermogravimetry and hot stage microscopy. Nanofibers with a smooth surface were generated at 0.2 MPa working pressure and those with a rough surface were generated without any working pressure. Porous PAN nanofibers were prepared by using PMMA as a sacrificial polymer. The 50:50 PAN-PMMA blend fibers were subjected to heat treatment to obtain porous fibers. The less thermally stable PMMA decomposes when heating, generating pores on the surface of the PAN fibers. The porous nanofibers have a higher surface area to volume ratio compared to smooth fibers, and these fibers could be useful in a variety of applications such as tissue engineering , filtering and purification.

Keywords: pressurized gyration, polymer, fiber, surface

*Corresponding Author: m.edirisinghe@ucl.ac.uk

1. Introduction

Nanofibers have attracted significant interest recently and have been used in different applications such as filter systems, biological sensors, scaffolds, transport media and textiles. These fibers possess unique characteristics such as high surface area to volume ratio, high rate of adsorption, low density and high surface volume [1]. The surface of the nanofibers can be functionalized in order to obtain the desired activity[2, 3] by using techniques such as vapour-phase atomic layer deposition treatment and surface grafting [3]. Their surface area can be further increased by introducing pores [4] and dimples [5] on the surface of the nanofibers. Single step fabrication of nanofibers with rough or porous surface is quite challenging in comparison to fibers with smooth surfaces as the processing parameters of conventional methods such as electrospinning, template synthesis, phase separation etc. are not able to easily modify the surface morphology of the fibers. Currently porous nanofibers are produced by controlling the spinning environment, the solution parameters and using sacrificial polymer/material[4, 6, 7]. Previous reports have shown that porous nanofibers have superior activity in terms of protein adsorption, cell proliferation, ultrafiltration [8-10] and electrical conductivity in comparison to fibers with smooth surfaces. Leong et al,[11] have shown that nanofibers with roughened and porous surfaces were able to adsorb 80% more protein than fibers with smooth surfaces. Zamani et al,[12] have compared the growth and proliferation of nerve cell on roughened and smooth surfaces, and found that porous and roughened surfaces showed higher cell adhesion.

Nanofibers can be prepared by using various techniques such as phase separation [13], template synthesis [14], self-assembly [15] and electrospinning[16, 17]. Among these techniques electrospinning is the most popular technique, but it has crucial disadvantages such as low production rate, utilization of very high voltage (kV range) and sensitivity to dielectric constant of the polymer solution. Further, during electrospinning the polymer jet carries a surface charge induced by the high voltage, and this charge persists until at least the jet meets the fiber collector. Therefore, it is harder to modify the surface of the fiber during fabrication. The above-mentioned limitations demand a novel cost effective technique to fabricate nanofibers with high production rate. Recently discovered pressurised gyration is a simple and cost effective technique which can generate nanofibers at high production rate [18]. Since 2013, this technique has been widely used to prepare nanofibers from various polymers for different applications such as drug delivery and tissue engineering[18-21]. The pressurized gyration has been further developed as infusion gyration [22] and pressurized melt gyration [23] to cater for a wider variety of solutions as well as to polymer melts. In infusion gyration the polymer solution is fed to the gyration vessel at a constant rate using a syringe pump instead of placing the polymer solution in the gyration vessel. This allows continues production of fibers. In the melt gyration, polymer granules are placed in the gyration vessel. Then while gyrating the temperature of the gyration vessel is increased by using an external heating gun until the polymer melts. Fibers from melt gyration are more suitable for biomedical application as this process does not utilise solvents. There is scope to increase the diameter and height of the gyration vessel to sustain higher working pressure and rotation speed. The fiber yield can be increased by increasing the number of pin-hole outlets and their diameter. This work is currently in progress in our laboratory.

The pressurised gyration method utilizes centrifugal spinning and solution blowing simultaneously to produce nanofibers. The gyration set up consist of a rotary aluminium vessel which contain of a series of pin-hole type orifices (0.5 mm in diameter) on its circumference and the top of the vessel is connected to a gas cylinder which is capable of producing pressure up to 3×10^5 Pa, and at the bottom to a DC motor – which is used to rotate the vessel, and to a speed controller to set the rotation speed up to a maximum of 36000 rpm. The polymer solution is placed in the vessel and, during gyration, when the centrifugal force exceeds the surface tension of the polymer solution a jet is ejected through each orifice. The polymer jet stretches due to centrifugal force and pressure difference, and travels through the air and is deposited on the collector. During jetting, the solvents evaporate and solid nanofibers are formed. The fiber formation during the gyration process can be explained by the Rayleigh−Taylor instability [24] of the polymer solution jet emerging from the orifice of the gyration vessel. The fiber diameter and morphology can be changed by varying the polymer concentration, rotation speed of the vessel and the working pressure[18-21]. Recent work showed that this technique is also able to produce microbubbles by carefully controlling the rotation speed and applied pressure[25].

Polymer blending is one of the most widely used methods to generate porous nanofibers [26-29]. In this work, two immiscible polymers, polyacrylonitrile (PAN) and polymethylmethacrylate (PMMA) have been used to generate porous nanofibers. PAN is a well-known polymer used in various applications such as water treatment [30], drug delivery [31, 32] and many other biomedical applications [33]. Also PAN has good film forming properties and is used as a precursor to produce carbon nanofibers [34] . PAN nanofibers were previously prepared by using other fabricating techniques like electrospinning [35-37] and centrifugal spinning [38, 39]. PMMA is a thermoplastic polymer widely used in different fields such as biomedical [40-42], water purification [43] and textiles [44]. PMMA was selected as the pore forming agent in this study due to its low thermal stability. Upon decomposition, PMMA does not produce any carbon residues but only volatile compounds [45]. Porous PAN fibers have been previously obtained by several researchers using PMMA as the sacrificial polymer [7, 46, 47].

The aim of this work was to produce nanofibers with different surface morphologies, such as smooth, rough and porous using pressurized gyration. There is no recorded literature on gyrospun fibers with different surface morphologies and these fibers could be used in a wide range of applications, spanning textiles to the biomedical engineering. It should be noted that in the present work there was no dedicated attempt to study the internal structure of the fiber and investigations were focused on the fiber surface.

2. Materials and methods

2.1 Materials

Polyacrylonitrile (Mw 150 000 g/mol), Poly(methylmethacrylate) (Mw 120 000 g/mol) and *N*,*N*-dimethylformamide (DMF) were obtained from Sigma- Aldrich (Gillingham, UK). All reagents were analytical grade and were used as received.

2.2 Preparation of spinning solutions

DMF was selected as the solvent for this study as both PAN and PMMA show good solubility in DMF, and DMF rapidly evaporates during the forming process. 4%, 8% and 10% (w/v) PAN solutions were prepared by dissolving the appropriate amount of PAN in DMF and mixing using a magnetic stirrer for 48 hours. The polymer solutions were labelled as S1, S2 and S3 respectively. 30 % (w/v) PMMA solutions were prepared by dissolving the required amount of polymer in DMF while stirring for 24 hours. The resultant solution was labelled as S4. A separate spinning solution was prepared by mixing an equal amount of PAN and PMMA in DMF under stirring for 48 hours. The total polymer content of the solution was 20% (w/v), and it was labelled as S5.

2.3 Pressurised gyration process

A schematic diagram of the gyration apparatus is shown in Figure 1. The rotary aluminium cylindrical vessel (~ 60 mm in diameter and ~35 mm in height) contains 24 orifices on its face, each having a diameter of 0.5 mm. During the gyration process, 4 ml of the polymer solution was placed in the vessel and spun at 36000 rpm. Two different sets of PAN fibers were prepared, one without any applied pressure and the other with 0.2 MPa applied pressure. The fibers were collected using a rod - collector placed 100 mm way from the vessel. All the spinning experiments were carried out under ambient condition (22 ± 3 °C and relative humidity 40 ± 3%).

2.4 Fiber characterisation

2.4.1 Scanning electron microscopy (SEM)

The fiber morphology was assessed using a scanning electron microscope (Quanta 200 FEG ESEM, FEI, Hillsborough, OR, USA). Prior to imaging, the samples were coated with 20 nm of gold under argon using a Quorum Q150T turbo-pumped sputter coater. All the SEM images were taken at an acceleration voltage of 5 kV. The average fiber diameter was determined by measuring the diameter of more than 50 fibers captured by SEM images in using ImageJ software (National Institute of Health, Bethesda, MD, USA). The fiber diameters of the generated fibers are given in Table 1.

2.4.1 Hot stage microscopy

Hot stage microscopy was carried out using a LeicaDML52 microscope with a x10 magnification lens connected to a Mettler Toledo FP90 hot stage. Each sample was placed on a microscope slide, contained with a cover-slip and heated at 5 ^{0}C min $^{-1}$ from 37 ^{0}C to 300 ^{0}C. Resulting thermal events were recorded in real time using Studio86 Design capture software (version 4.0.1).

2.4.2 Thermogravimetric analysis (TGA)

Thermogravimetric analysis were carried out for PMMA, PAN, 50:50 PMMA-PAN blend fibers under nitrogen at a flow rate of 50 ml min^{-1} using a TA Instruments SDT Q600 Analyzer at a heating rate of 10 ˚C min^{-1}, from ambient temperature to 600 ˚C using a platinum sample pan.

2.5 Heat treatment

S3 and S5 fibers were subjected to heat treatment in a standard carbolite tube furnace. Initially, all the samples were heated at a 2 ^{0}C min $^{-1}$ up to 300 ^{0}C in air, and subsequently temperature was increased to 400 ^{0}C under nitrogen (99.99% purity) at a 2 ^{0}C min $^{-1}$. The heat treated fibers were imaged using the SEM to study their surface morphology.

3. Results and discussion

3.1 Fiber morphology

In this work rotation speed, which is one of the two main process control parameters of gyration spinning was kept constant at 36000 rpm. The other parameter, applied working pressure was varied between 0 – 0.2 MPa. Initially, S1 – S3 solutions were spun without any applied pressure at 36000 rpm. Without any applied pressure, solution S1 (4% (w/v PAN) was unable to produce any fibers and only polymer droplets formed (Figure 2a). However when increasing the pressure up to 0.2 MPa, some short length fibres (410±130 nm) were produced as shown in Figure 3a1. But even at 0.2 MPa, most of the S1 solution sprayed out as droplets. This is because at a low polymer concentration (S1) there is insufficient chain entanglements to produce continuous fibers. However, it is clear from the experimental observation that the applied pressure helps to generate fibers at low concentration by enhancing chain entanglement as well as by jet elongation. The high speed air flow creates turbulence in the rotating vessel and forcefully pushes the polymer solution through the orifices. Without applied pressure it is only the centrifugal force that pushes the polymer solution out of the orifices, and this is not sufficient to produce continues fibers with low concentration solutions. Higher magnification SEM images of S1 fibers shows that these fibers have a smooth surface (Figure 3a1).

Both S2 and S3 were able to produce fibers without any applied pressure although, some droplets were also generated. Interestingly, the surface of these fibers contained a rough surface (Figure 2b1, 2c1) in comparison to fibers produced under 0.2 MPa applied pressure (Figure 3b1, 3c1). This is because, without any pressure, the solvent (DMF) evaporates under normal atmospheric conditions. When pressure is applied, the high speed air flow increases the rate of DMF evaporation from the polymer jet, creating fibers with smooth surfaces. However, it was evident that the fiber production rate at 0 MPa is considerably low in comparison to that obtained at 0.2 MPa. The diameter of the fibers produced under pressure was 520 ±180and 450 ±150 nm for samples from solution S2 and S3, respectively.

S4 solution was spun at 36000 rpm at 0 MPa and 0.2 MPa. Similar to PAN fibers, the PMMA fibers obtained at 0 MPa contained a rough surface (Figure 2d1) while the fibers obtained with 0.2MPa had a smooth surface (Figure 3d1). The average fiber diameter of the S4 fibers was 290 ±80 nm. Thus, S4 fibers were smaller in diameter in comparison to S2 and S3 fibers. A similar observation was recorded in the centrifugal spinning work of Lu et al [47] ., who made porous carbon fibers by using PAN and PMMA. The fibers produced without any applied pressure from S5 contained rough surfaces, as shown in Figure 2e1. S5 fibers generated using 0.2 MPa applied pressure also had rough surfaces (Figure 3e1), and fiber diameter was bimodally distributed. It seems that the blended polymer solution S5 also generated individual PAN and PMMA fibers, in addition to blend fibers. The thinner fibers shown in Figure 3e1 can be attributed to PMMA while the thicker fibers are likely to be PAN fibers, based on fiber diameter of individual fibers. The surface tension of the PAN solutions are lower in comparison to PMMA [45]. Due to this surface tension difference, the blend polymer solution can form islands in the microstructure [45]. The lower surface tension component (PAN) forms the continuous phase and the higher surface tension component (PMMA) forms droplets. Due to the centrifugal force and applied pressure these PMMA droplets get stretched and elongated when extruded through the orifices in the gyration vessel. Elongated PMMA droplets are present on the surface of the PAN fibers creating a rough surface on blend fibers even at 0.2 MPa applied pressure. These observations clearly demonstrate that most spinning solutions were able to produce fibers with rough surfaces without any pressure in the gyration process. Compared to electrospinning an added advantage in the pressurized gyration is that, the polymer jet is charge-free. This allows production of fibers with a smooth surface or a rough surface upon demand by varying working pressure.

3.2 Thermal behaviour

Hot stage microscopy was performed in order to observe the thermal behaviour of the fibers. Figure 4a1 –a3 shows the thermal behaviour of the S3 fibers. When the temperature increased S3 fibers start to shrink. The cyclization of nitrile groups in PAN occurs in the 250 to 300 ^{0}C temperature range [34] and this could be the reason for shrinkage of fibers at a higher temperature. A similar observation was reported by Sarvaranta [48]. Even at 300 ^{0}C it is evident that S3 fibers were present on the glass slide (Figure 4a3). Similarly S4 fibers were heated up to 300 ^{0}C and their thermal behaviour was investigated. The glass transition temperature (Tg) of commercial grade PMMA varies from 85 to 165 ^{0}C [49, 50]. It was observed that between

150 to 175 ^{0}C, S4 fibers showed bending and stretching movements and at 300 ^{0}C all the S4 fibers decomposed, and there was no fibers were visible under the microscope (Figure 4c3). S5 blended fibers, showed more interesting thermal behaviour under hot stage microscopy (see video included as supporting data). When heating S5 fibers, at 150 – 175 ^{0}C some fibers started to show bending and stretching movements, while other fibers did not show any movements. It is very clear from the video data that the fibers did not show any bending and stretching movements after 250 ^{0}C. Also, it is evident from the SEM image of S5 fibers that gyration resulted in the production of both thin and thick fibers. Therefore, we can assign the moving fibers to PMMA that where individually spun during the gyration process. These PMMA fibers in the S5 sample cannot be visualized after 250 ^{0}C, and the remaining fibers show shrinkage due to decomposition of PMMA in the fibers and well as due to cyclization of their nitrile groups.

The thermal decomposition behaviour of the fabricated fibers were investigated using TGA. PAN fibers (S3) showed a sharp weight loss in the 300 - 450 ˚C temperature range. When heating the PAN fibers, volatile by-products such as CO_2, HCN, water vapour are produced[51, 52] leading to a weight loss. Pure PMMA fibers (S4) start to decompose at 250 ˚C. After 250 ˚C, S4 fibers undergo an intrinsic degradation process incorporating depolymerizaton, random scission and side group elimination with the creation of volatile compounds. Previous reports show that PMMA degrades to its monomer over a narrow temperature window (250 - 400 ˚C) without leaving any carbon residue [53]. Therefore, no residue of PMMA is present after 400 ˚C. This was visualized in the hot stage microscopy experiment with S4 fibers.

In S5 blend fibers, the weight loss mainly occurred in two temperature ranges: 225 - 300 ˚C and 300 - 475 ˚C. The first weight loss can be attributed to the cyclization of nitrile group in PAN and the second weight loss corresponds to PMMA decomposition. When PMMA decomposes, volatile degradation products (e.g monomers) and residual solvents penetrate through the PAN shell and evaporate at the surface of the PAN fibers.

3.3 Heat Treated fibers

S3 and S5 fiber were subjected to heat treatment. The SEM images of the heat treated fibers are given in Figure 6. It is clear from Figures 6a and 6a1 that heat treated S3 fibers have smooth surfaces and heat treated S5 fibers have pores on the surface of the fibers. Even though S3 fibers produce volatile products while heating, this gas release does not alter the surface morphology of S3 fibers. It is quite clear from Figure 3e1 that as-spun S5 blended fibers have elongated PMMA droplets on the surface of the fiber. After heat treatment, those elongated PMMA droplets disappear due to PMMA decomposition while creating similar shape pores on the surface of the fibers.

4. Conclusions

Polymeric nanofibers with smooth, rough and porous surfaces were produced using pressurized gyration. It was uncovered that the applied pressure playing a major role in the gyration process to generate fibers with different surface morphologies. The PAN, PMMA and 50:50 PAN-PMMA blend fibers produced with 0 MPa working pressure gave fibers with rough surfaces, while the fibers produced using 0.2 MPa had smooth surfaces except for the blend fibers. In these blend fibers, the matrix seems to be PAN, while PMMA was present as isolated islands throughout the fibers. Porous fibers were produced by heating 50:50 PAN-PMMA blend fibers. During the heating process, the less thermally stable PMMA decomposed completely leading to the formation of pores evenly distributed on the fiber surface. The porous and rough surface fibers have higher surface area in comparison to the fibers with smooth surfaces. These fibers with variable surface morphology could be used in a wider range of applications compared with conventional smooth fibers, spanning textiles to tissue engineering.

Acknowledgement

The authors would like to thank Mr David McCarthy (University College London School of Pharmacy) for his assistance with the FEI™ Quanta 200F Field Emission Scanning Electron Microscope, Mr Jalil Muhaammad for his assistance with hot stage microscopy and Dr. Asma Buanz for her assistance with TGA.

References

1. Luo CJ, Stoyanov SD, Stride E, Pelan E, Edirisinghe M (2012) Electrospinning versus fibre production methods: from specifics to technological convergence. *Chemical Society Reviews* 41(13):4708-4735.
2. Wang P, Wang Y, Tong L (2013) Functionalized polymer nanofibers: a versatile platform for manipulating light at the nanoscale. *Light Sci Appl* , doi:10.1038/lsa.2013.58.
3. Cortese B, Caschera D, Padeletti G, Ingo GM, Gigli G (2013) A brief review of surface-functionalized cotton fabrics. *Surface Innovations* 1(3):140-156.
4. Megelski S, Stephens JS, Chase DB, Rabolt JF (2002) Micro- and nanostructured surface morphology on electrospun polymer fibers. *Macromolecules* 35(22):8456-8466.
5. Deitzel JM, Kleinmeyer J, Harris D, Beck Tan NC (2001) The effect of processing variables on the morphology of electrospun nanofibers and textiles. *Polymer* 42(1):261-272.
6. Casper CL, Stephens JS, Tassi NG, Chase DB, Rabolt JF (2004) Controlling Surface Morphology of Electrospun Polystyrene Fibers: Effect of Humidity and Molecular Weight in the Electrospinning Process. *Macromolecules* 37(2):573-578.
7. Abeykoon NC, Bonso JS, Ferraris JP (2015) Supercapacitor performance of carbon nanofiber electrodes derived from immiscible PAN/PMMA polymer blends. *Rsc Advances* 5(26):19865-19873.
8. Moon S, Choi J, Farris RJ (2008) Highly porous polyacrylonitrile/polystyrene nanofibers by electrospinning. *Fibers and Polymers* 9(3):276-280.
9. Zhang L, Hsieh Y-L (2006) Nanoporous ultrahigh specific surface polyacrylonitrile fibres. *Nanotechnology* 17(17):4416-4423.
10. Kumakura M. (2001) Preparation method of porous polymer materials by radiation technique and its application. *Polymers for Advanced Technologies* 12(7):415-421.
11. Leong MF, Chian KS, Mhaisalkar PS, Ong WF, Ratner BD (2009) Effect of electrospun poly(D,L-lactide) fibrous scaffold with nanoporous surface on attachment of porcine esophageal epithelial cells and protein adsorption. *Journal of Biomedical Materials Research Part A* 89A(4):1040-1048.
12. Zamani F, Amani-Tehran M, Latifi M, Shokrgozar MA. The influence of surface nanoroughness of electrospun PLGA nanofibrous scaffold on nerve cell adhesion and proliferation (2013) *Journal of Materials Science: Materials in Medicine* 24(6):1551-1560.
13. Zhao J, Han W, Chen H, Tu M, Zeng R, Shi Y, et al. (2011) Preparation, structure and crystallinity of chitosan nano-fibers by a solid–liquid phase separation technique. *Carbohydrate Polymers* 83(4):1541-1546.
14. Tao SL, Desai TA (2007) Aligned Arrays of Biodegradable Poly(ε-caprolactone) Nanowires and Nanofibers by Template Synthesis. *Nano Letters* 7(6):1463-1468.
15. O'Leary LER, Fallas JA, Bakota EL, Kang MK, Hartgerink JD (2011) Multi-hierarchical self-assembly of a collagen mimetic peptide from triple helix to nanofibre and hydrogel. *Nat Chem* 3(10):821-828.
16. Illangakoon UE, Gill H, Shearman GC, Parhizkar M, Mahalingam S, Chatterton NP, et al (2014) Fast dissolving paracetamol/caffeine nanofibers prepared by electrospinning. *International Journal of Pharmaceutics* 477(1–2):369-379.
17. Sofokleous P, Stride E, Edirisinghe M (2013) Preparation, characterization, and release of amoxicillin from electrospun fibrous wound dressing patches. *Pharmaceutical research* 30(7):1926-1938.
18. Mahalingam S, Edirisinghe M (2013) Forming of Polymer Nanofibers by a Pressurised Gyration Process. *Macromolecular Rapid Communications* 34(14):1134-1139.
19. Raimi-Abraham BT, Mahalingam S, Davies PJ, Edirisinghe M, Craig DQM(2015) Development and Characterization of Amorphous Nanofiber Drug Dispersions Prepared Using Pressurized Gyration. *Molecular Pharmaceutics* 12(11):3851-3861.
20. Mahalingam S, Ren GG, Edirisinghe MJ (2014) Rheology and pressurised gyration of starch and starch-loaded poly(ethylene oxide). *Carbohydrate Polymers* 114:279-287.
21. Raimi-Abraham BT, Mahalingam S, Edirisinghe M, Craig DQM (2014) Generation of poly(N-vinylpyrrolidone) nanofibres using pressurised gyration. *Materials Science & Engineering C-Materials for Biological Applications* 39:168-176.
22. Zhang S, Karaca BT, VanOosten SK, Yuca E, Mahalingam S, Edirisinghe M, et al(2015) Coupling Infusion and Gyration for the Nanoscale Assembly of Functional Polymer Nanofibers Integrated with Genetically Engineered Proteins. *Macromolecular Rapid Communications* 36(14):1322-1328.
23. Xu Z, Mahalingam S, Basnett P, Raimi-Abraham B, Roy I, Craig D, et al (2016) Making Nonwoven Fibrous Poly(ε-caprolactone) Constructs for Antimicrobial and Tissue Engineering Applications by Pressurized Melt Gyration. *Macromolecular Materials and Engineering*, DOI: 10.1002/mame.201600116.
24. Sharp DH (1984) An overview of Rayleigh-Taylor instability. *Physica D* 12(1-3):3-18.
25. Mahalingam S, Raimi-Abraham BT, Craig DQM, Edirisinghe M (2015) Formation of Protein and Protein–Gold Nanoparticle Stabilized Microbubbles by Pressurized Gyration. *Langmuir* 31(2):659-666.
26. Peng M, Li D, Shen L, Chen Y, Zheng Q, Wang H (2006) Nanoporous structured submicrometer carbon fibers prepared via solution electrospinning of polymer blends. *Langmuir* 22(22):9368-9374.
27. Venugopal JR, Low S, Choon AT, Kumar AB, Ramakrishna S (2008) Nanobioengineered electrospun composite nanofibers and osteoblasts for bone regeneration. *Artificial Organs* 32(5):388-397.
28. You Y, Youk JH, Lee SW, Min BM, Lee SJ, Park WH (2006) Preparation of porous ultrafine PGA fibers via selective dissolution of electrospun PGA/PLA blend fibers. *Materials Letters* 60(6):757-760.
29. Zhang C, Bai Y, Sun Y, Gu J, Xu Y (2010) Preparation of hydrophilic HDPE porous membranes via thermally induced phase separation by blending of amphiphilic PE-b-PEG copolymer. *Journal of Membrane Science* 365(1-2):216-224.

30. Makaremi M, De Silva RT, Pasbakhsh P (2015) Electrospun Nanofibrous Membranes of Polyacrylonitrile/Halloysite with Superior Water Filtration Ability. *Journal of Physical Chemistry C* 119(14):7949-7958.
31. Balasubramanian K, Kodam KM (2014) Encapsulation of therapeutic lavender oil in an electrolyte assisted polyacrylonitrile nanofibres for antibacterial applications. *Rsc Advances* 4(97):54892-54901.
32. Yu D-G, Branford-White C, Li L, Wu X-M, Zhu L-M(2010) The Compatibility of Acyclovir with Polyacrylonitrile in the Electrospun Drug-Loaded Nanofibers. *Journal of Applied Polymer Science* 117(3):1509-1515.
33. Wang Z-G, Wan L-S, Xu Z-K (2007) Surface engineerings of polyacrylonitrile-based asymmetric membranes towards biomedical applications: An overview. *Journal of Membrane Science* 304(1–2):8-23.
34. Nataraj SK, Yang KS, Aminabhavi TM (2012) Polyacrylonitrile-based nanofibers—A state-of-the-art review. *Progress in Polymer Science* 37(3):487-513.
35. Ge JJ, Hou HQ, Li Q, Graham MJ, Greiner A, Reneker DH, et al (2004) Assembly of well-aligned multiwalled carbon nanotubes in confined polyacrylonitrile environments: Electrospun composite nanofiber sheets. *Journal of the American Chemical Society* 126(48):15754-15761.
36. Gu SY, Ren J, Vancso GJ (2005) Process optimization and empirical modeling for electrospun polyacrylonitrile (PAN) nanofiber precursor of carbon nanofibers. *European Polymer Journal* 41(11):2559-2568.
37. Borhani S, Hosseini SA, Etemad SG, Militky J (2008) Structural characteristics and selected properties of polyacrylonitrile nanofiber mats. *Journal of Applied Polymer Science* 108(5):2994-3000.
38. Dabirian F, Ravandi SAH, Pishevar AR (2013) The effects of operating parameters on the fabrication of polyacrylonitrile nanofibers in electro-centrifuge spinning. *Fibers and Polymers* 14(9):1497-1504.
39. Lu Y, Li Y, Zhang S, Xu G, Fu K, Lee H, et al (2013) Parameter study and characterization for polyacrylonitrile nanofibers fabricated via centrifugal spinning process. *European Polymer Journal* 49(12):3834-3845.
40. Wen J, Jiang F, Yeh C-K, Sun Y (2016) Controlling fungal biofilms with functional drug delivery denture biomaterials. *Colloids and Surfaces B-Biointerfaces* 140:19-27.
41. Lohmann CH, Dean DD, Koster G, Casasola D, Buchhorn GH, Fink U, et al (2002) Ceramic and PMMA particles differentially affect osteoblast phenotype. *Biomaterials* 23(8):1855-1863.
42. Tan H, Peng Z, Li Q, Xu X, Guo S, Tang T (2012) The use of quaternised chitosan-loaded PMMA to inhibit biofilm formation and downregulate the virulence-associated gene expression of antibiotic-resistant staphylococcus. *Biomaterials* 33(2):365-377.
43. Cantarella M, Sanz R, Buccheri MA, Ruffino F, Rappazzo G, Scalese S, et al (2016) Immobilization of nanomaterials in PMMA composites for photocatalytic removal of dyes, phenols and bacteria from water. *Journal of Photochemistry and Photobiology A: Chemistry* 321:1-11.
44. Alay S, Alkan C, Gode F (2011) Synthesis and characterization of poly(methyl methacrylate)/n-hexadecane microcapsules using different cross-linkers and their application to some fabrics. *Thermochimica Acta* 518(1-2):1-8.
45. Kim C, Jeong YI, Ngoc BTN, Yang KS, Kojima M, Kim YA, et al (2007) Synthesis and characterization of porous carbon nanofibers with hollow cores through the thermal treatment of electrospun copolymeric nanofiber webs. *Small* 3(1):91-95.
46. Li G, Xie T, Yang S, Jin J, Jiang J (2012) Microwave Absorption Enhancement of Porous Carbon Fibers Compared with Carbon Nanofibers. *Journal of Physical Chemistry C* 116(16):9196-9201.
47. Lu Y, Fu K, Zhang S, Li Y, Chen C, Zhu J, et al (2015) Centrifugal spinning: A novel approach to fabricate porous carbon fibers as binder-free electrodes for electric double-layer capacitors. *Journal of Power Sources* 273:502-510.
48. Sarvaranta L (1995) Shrinkage of short PP and PAN fibers under hot stage microscopy. *Journal of Applied Polymer Science* 56(9):1085-1091.
49. Kuo S-W, Kao H-C, Chang F-C (2003) Thermal behavior and specific interaction in high glass transition temperature PMMA copolymer. *Polymer* 44(22):6873-6882.
50. Porter CE, Blum FD (2000) Thermal characterization of PMMA thin films using modulated differential scanning calorimetry. *Macromolecules* 33(19):7016-7020.
51. Hanna SB, Yehia AA, Ismail MN, Khalaf AI (2012) Preparation and Characterization of Carbon Fibers from Polyacrylonitrile Precursors. *Journal of Applied Polymer Science* 123(4):2074-2083.
52. Rahaman MSA, Ismail AF, Mustafa A (2007) A review of heat treatment on polyacrylonitrile fiber. *Polymer Degradation and Stability* 92(8):1421-1432.
53. Zussman E, Yarin AL, Bazilevsky AV, Avrahami R, Feldman M (2006) Electrospun polyacrylonitrile/poly (methyl methacrylate)-derived turbostratic carbon micro-/nanotubes. *Advanced Materials* 18(3):348-353.

List of figures and Table

Table 1. Diameter of fibers made from each formulation using 0.2 MPa working pressure. The rotation speed was kept constant at 36000 rpm

Fiber sample	Fiber diameter (nm)
S1	410 ±130
S2	520 ±180
S3	450 ±150
S4	290 ±80
S5	580 ±260

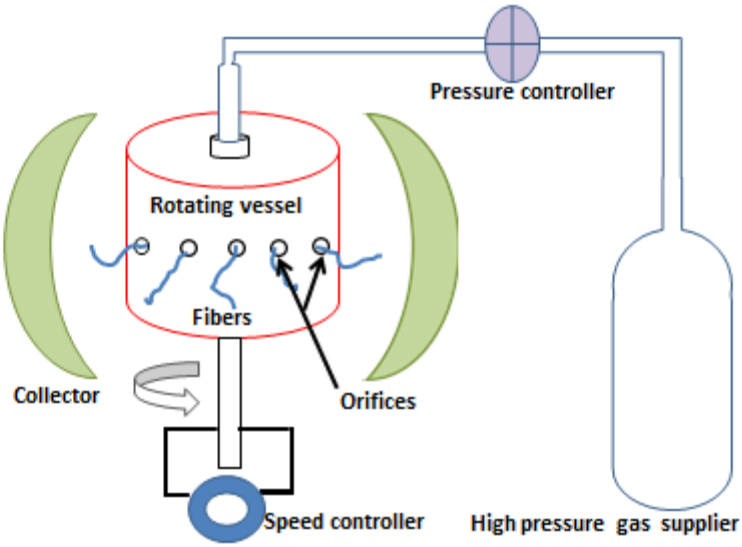

Figure 1. Schematic diagram of pressurized gyration apparatus

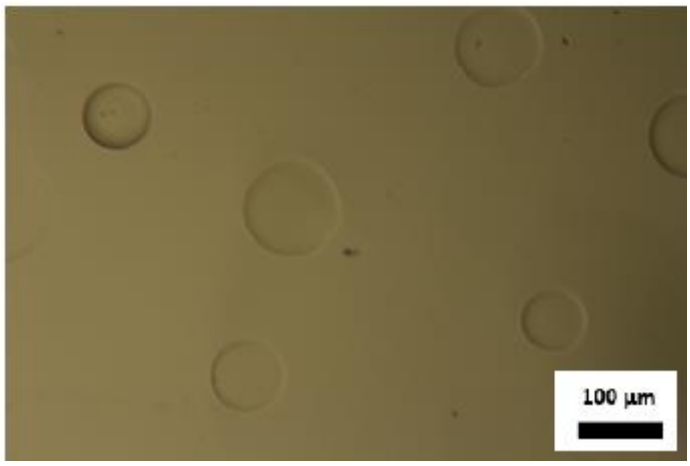
100 µm

(a)

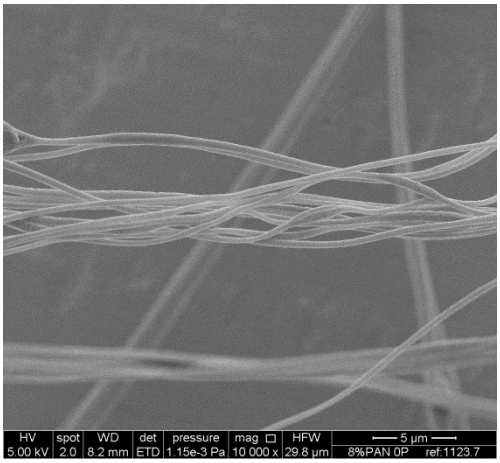
HV spot WD det pressure mag HFW 5 µm
5.00 kV 2.0 8.2 mm ETD 1.15e-3 Pa 10 000 x 29.8 µm 8%PAN 0P ref:1123.7

(b)

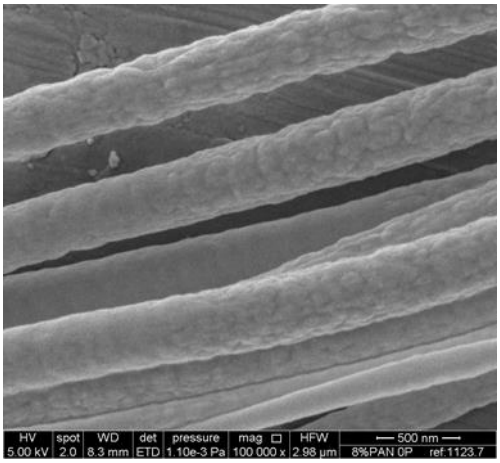
HV spot WD det pressure mag HFW 500 nm
5.00 kV 2.0 8.3 mm ETD 1.10e-3 Pa 100 000 x 2.98 µm 8%PAN 0P ref:1123.7

(b1)

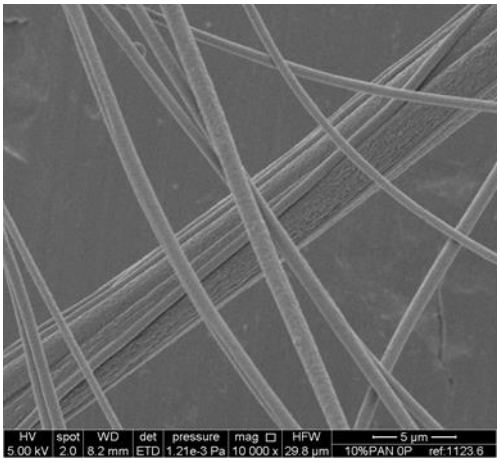
HV spot WD det pressure mag HFW 5 µm
5.00 kV 2.0 8.2 mm ETD 1.21e-3 Pa 10 000 x 29.8 µm 10%PAN 0P ref:1123.6

(c)

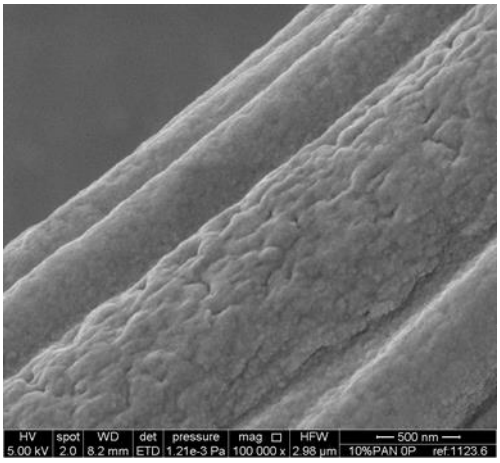
HV spot WD det pressure mag HFW 500 nm
5.00 kV 2.0 8.2 mm ETD 1.21e-3 Pa 100 000 x 2.98 µm 10%PAN 0P ref:1123.6

(c1)

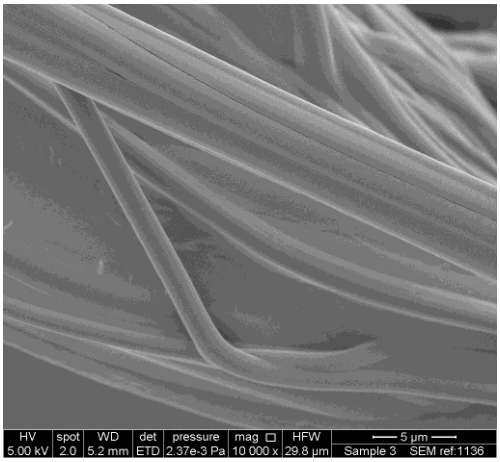

(d)

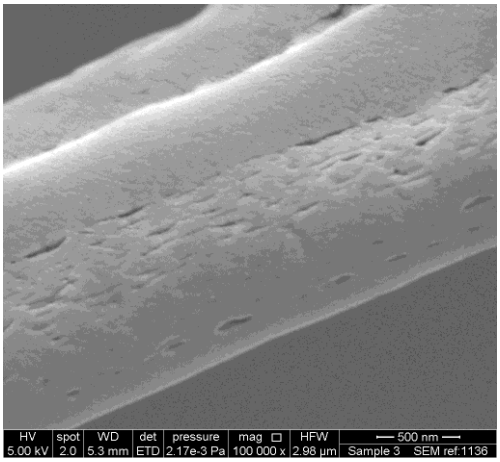

(d1)

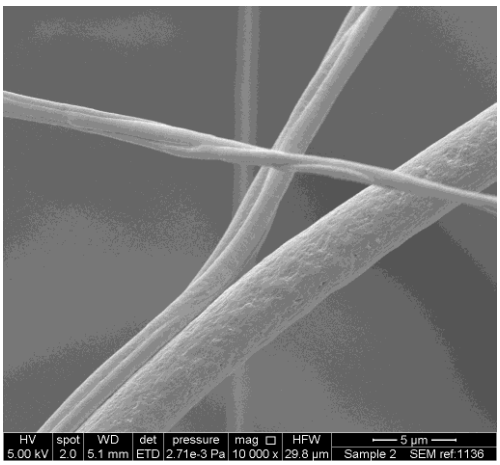

(e)

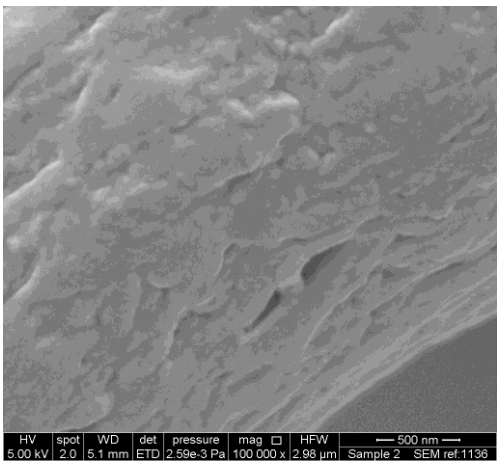

(e1)

Figure 2. (a) Optical micrograph of the droplets formed from S1 solution. Scanning electron micrographs of the gyrospn fibers made without the applied pressure: (b – e) S2,S3,S4 and S5 fibers at x 10000 magnification and (b1 – e1)) S2,S3,S4 and S5 fibers at x 100000 magnification.

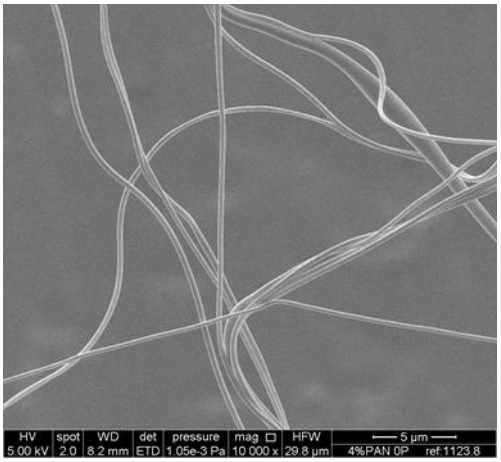
HV spot WD det pressure mag HFW 5 µm
5.00 kV 2.0 8.2 mm ETD 1.05e-3 Pa 10 000 x 29.8 µm 4%PAN 0P ref:1123.8

(a)

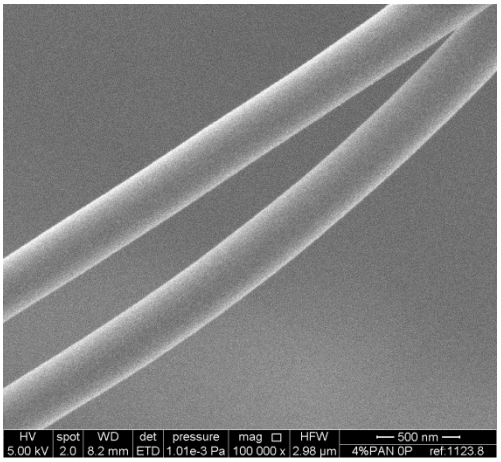
HV spot WD det pressure mag HFW 500 nm
5.00 kV 2.0 8.2 mm ETD 1.01e-3 Pa 100 000 x 2.98 µm 4%PAN 0P ref:1123.8

(a1)

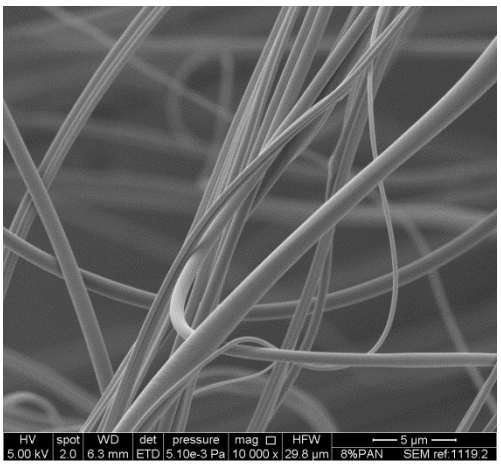
HV spot WD det pressure mag HFW 5 µm
5.00 kV 2.0 6.3 mm ETD 5.10e-3 Pa 10 000 x 29.8 µm 8%PAN SEM ref:1119.2

(b)

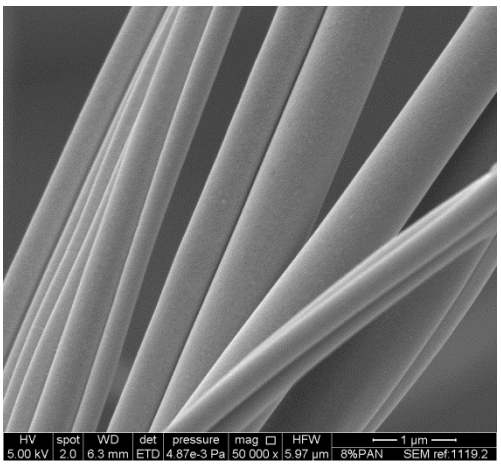
HV spot WD det pressure mag HFW 1 µm
5.00 kV 2.0 6.3 mm ETD 4.87e-3 Pa 50 000 x 5.97 µm 8%PAN SEM ref:1119.2

(b1)

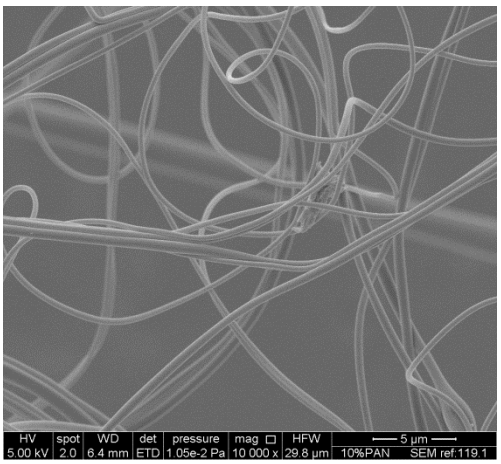
HV spot WD det pressure mag HFW 5 µm
5.00 kV 2.0 6.4 mm ETD 1.05e-2 Pa 10 000 x 29.8 µm 10%PAN SEM ref:119.1

(c)

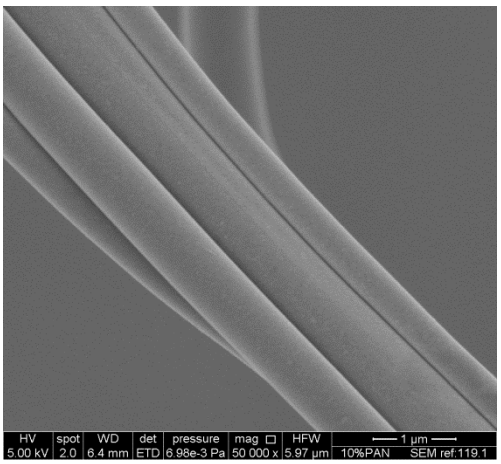
HV spot WD det pressure mag HFW 1 µm
5.00 kV 2.0 6.4 mm ETD 6.98e-3 Pa 50 000 x 5.97 µm 10%PAN SEM ref:119.1

(c1)

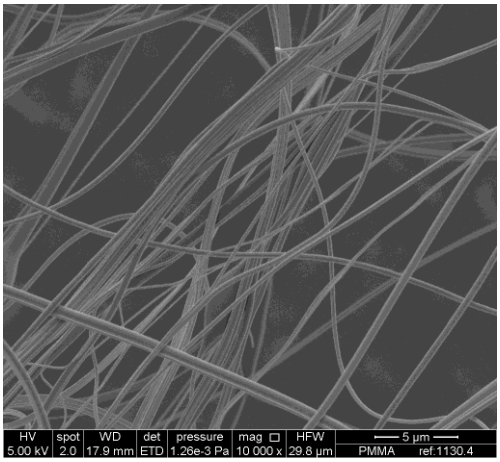

(d)

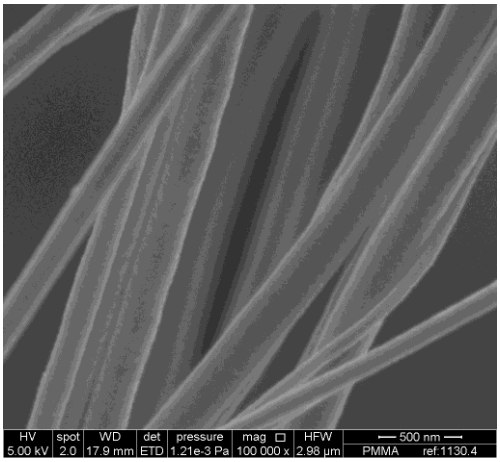

(d1)

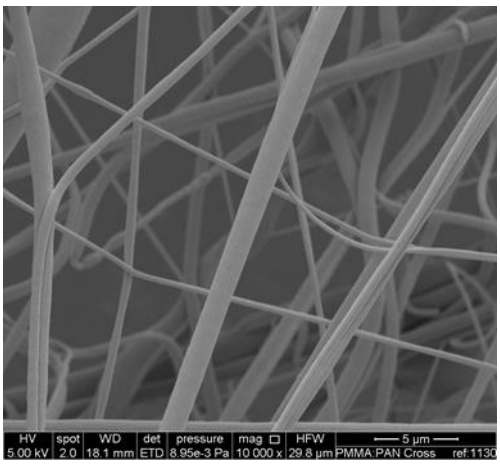

(e)

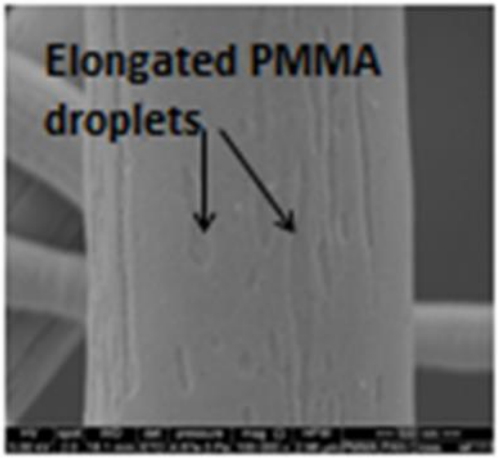

(e1)

Figure 3. Scanning electron micrographs of fibers made using 0.2 MPa applied pressure. (a – e) S1,S2,S3,S4 and S5 fibers at x 10000 magnification and (a1 – e1)) S1,S2,S3,S4 and S5 fibers at x 100000 magnification.

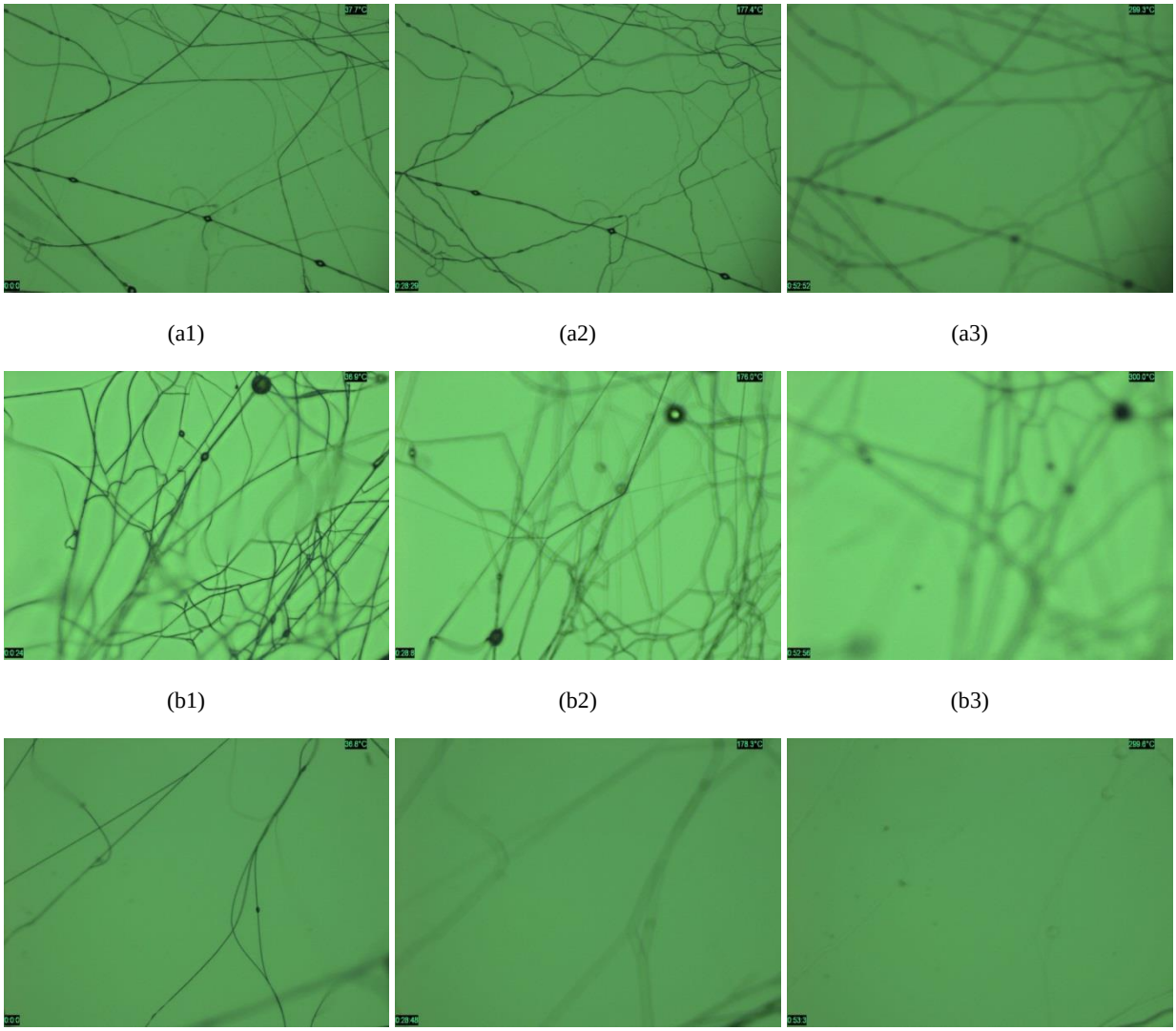

(a1) (a2) (a3)

(b1) (b2) (b3)

(c1) (c2) (c3)

Figure 4. A sequence of hot stage microscopy (also see video included in supplementary data) images (magnification x10) of S3,S5 and S4 fibers at 37 ˚C (a1,b1,c1), 175 ˚C (a1,b1,c1), 300 ˚C (a1,b1,c1), respectively.

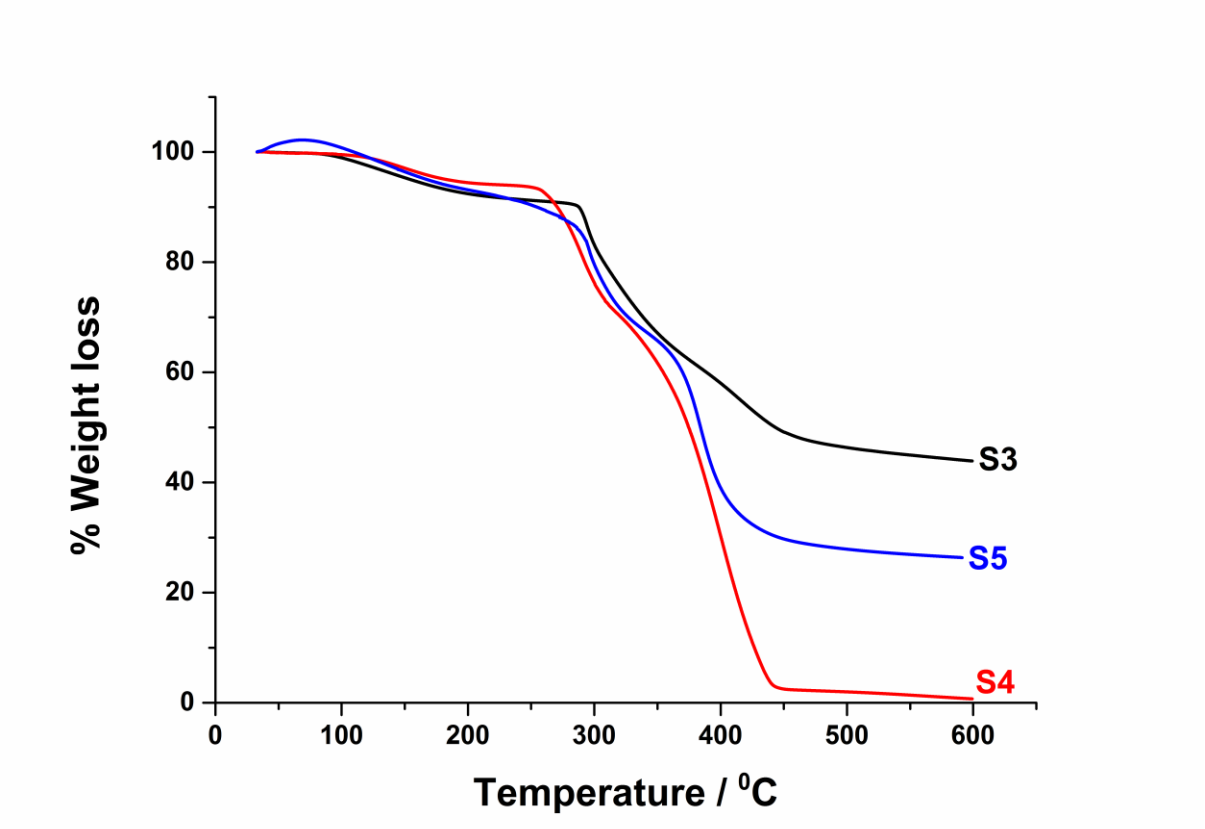

Figure 5. Thermogravimetric trace of fibers: S3 (PAN), S4 (PMMA) and S5 (PAN-PMMA blend fibers)

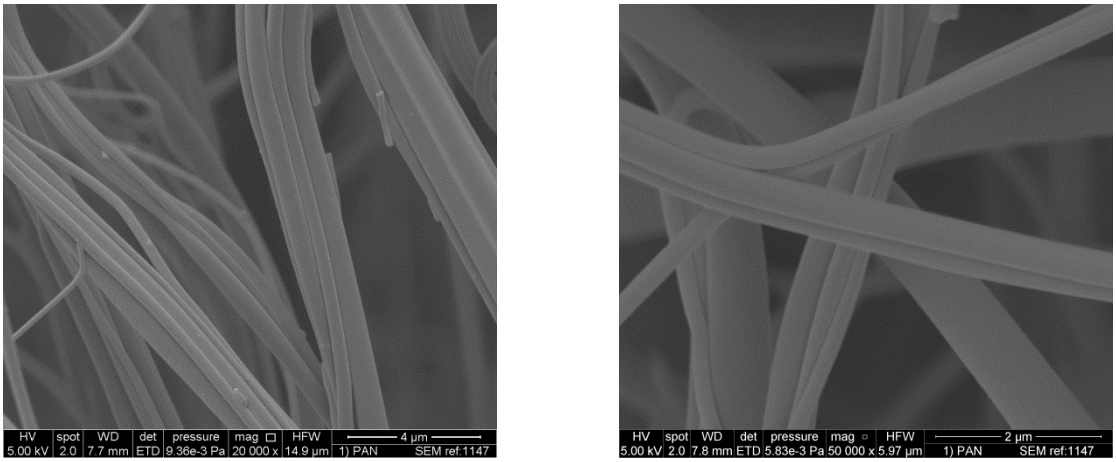

(a) (a1)

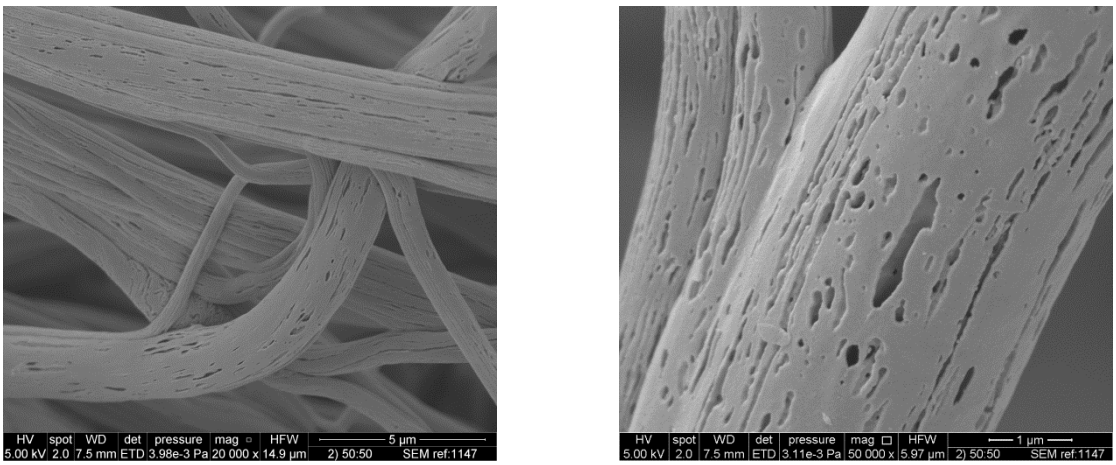

(b) (b1)

Figure 6. Scanning electron micrographs of heat treated S3 fibers (a- x20000, a1 - x100000) and S5 fibers (b- x20000, b1 - x100000)

Author Photos

Author Photos

Author Photos

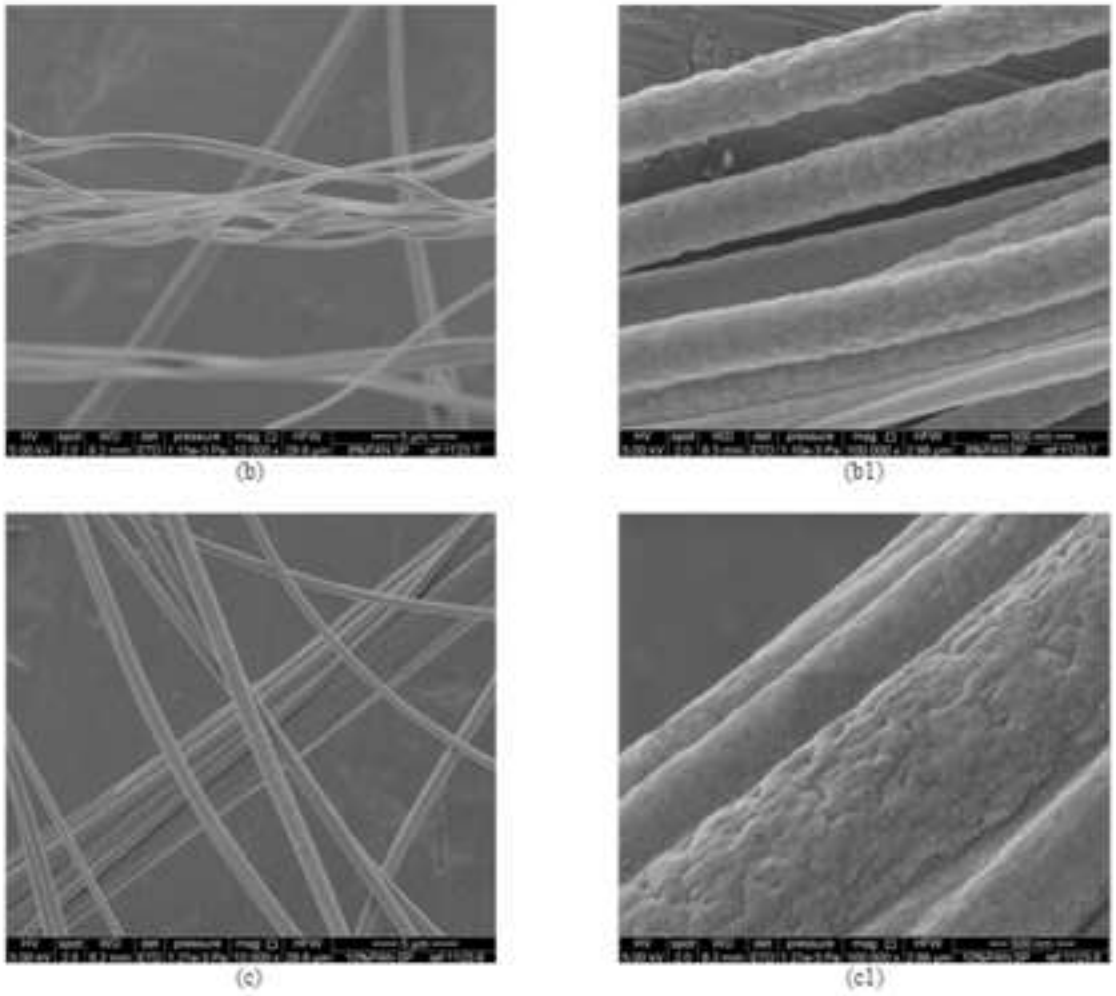

Author Photos

Figure 1

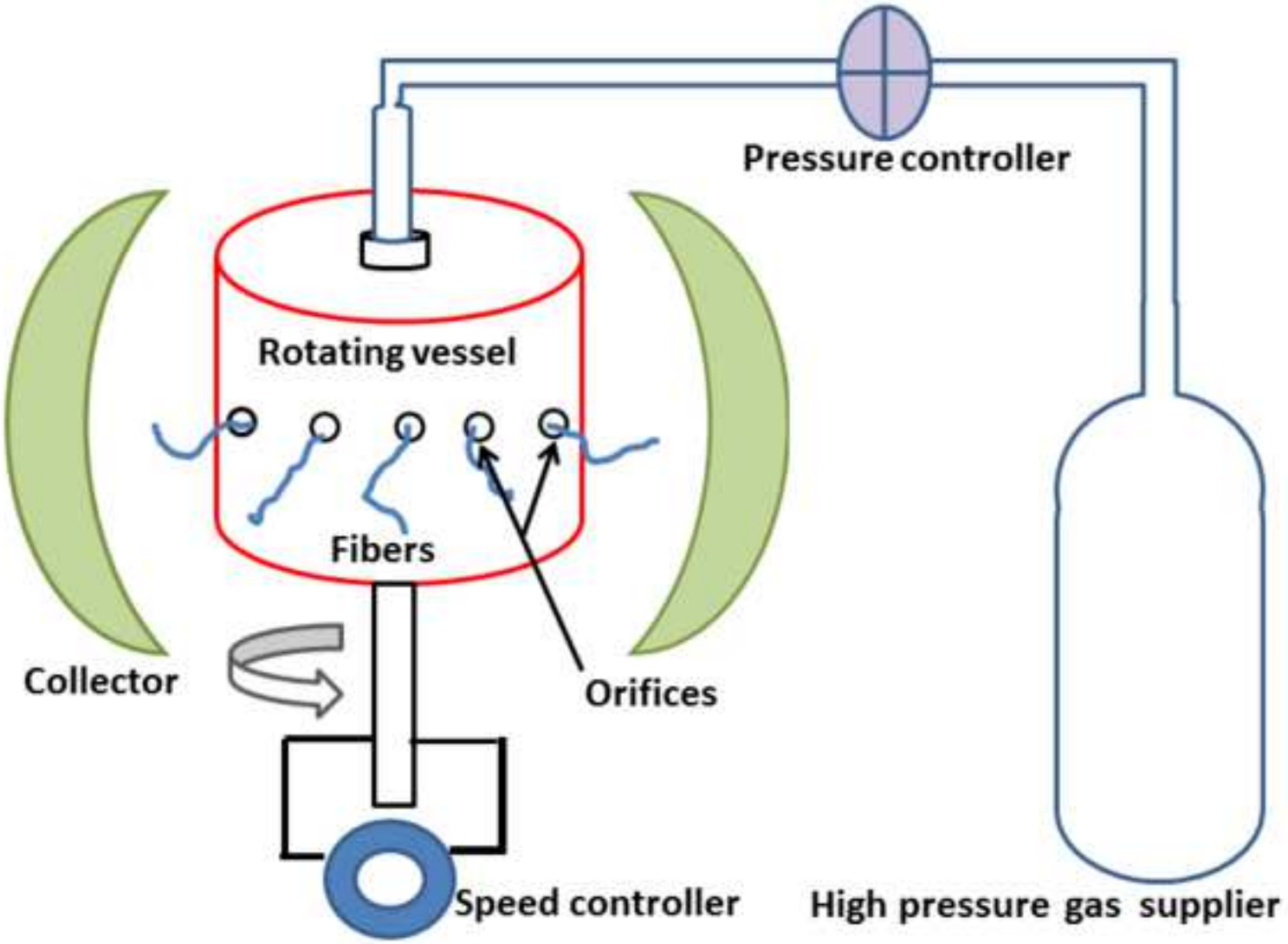

Figure 1

Click here to download Figures and line artwork Figure 2a.TIF

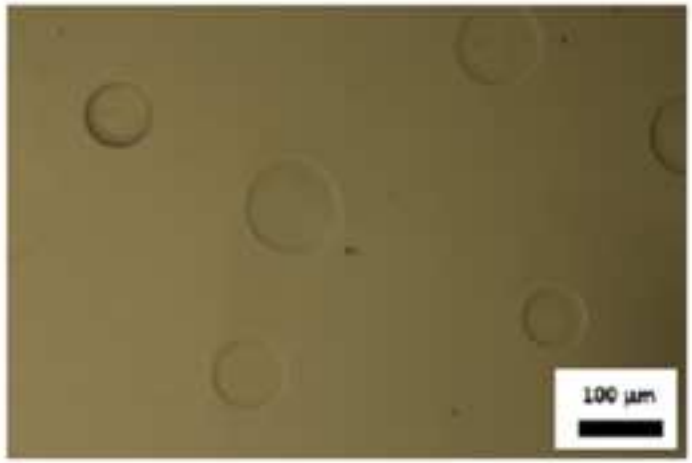

Journal Publishing Agreement

It is our policy to ask authors to assign the copyright of articles accepted for publication to the Publisher. Exceptions are possible for reasons of national rules or funding. Please tick the relevant options below.

In assigning copyright to us, you retain all proprietary rights including patent rights, and the right to make personal (non-commercial) use of the article, subject to acknowledgement of the journal as the original source of publication.

By signing this agreement, you are confirming that you have obtained permission from any co-authors and advised them of this copyright transfer. Kindly note that copyright transfer is not applicable to authors who are opting to publish their papers as Open Access. Open Access authors retain copyright of their published paper.

Please complete the form below and return an electronic copy to your ICE Publishing contact: (http://www.icevirtuallibrary.com/info/submit).

Journal name: SURFACE INNOVATIONS

Article title: Tailoring the surface of polymeric nanofibers - Generated by pressurized gyration.

Manuscript reference number: SURI-D-16-00007R1

Authors: UL ISLAM NAKOON SUNTHAR MAHALINGAM, PAOLO COLOMBO, MOHAN EDIRISINGHE

Your name: MOHAN EDIRISINGHE

Signature and date: MOHAN 11/07/2016

Please tick either one option from part A or one option from part B. Please complete part C.

A. Copyright

☑ I hereby assign and transfer the copyright of this paper to Thomas Telford Ltd.

☐ British Crown Copyright: I hereby assign a non-exclusive licence to publish to Thomas Telford Ltd.

☐ I am a US Government employee: employed by (name of agency) .....

☐ I am subject to the national rules of (country) ..... and confirm that I meet their requirements for copyright transfer or reproduction (please delete as appropriate)

B. Authors with open access funding requirements. Please specify the Creative Commons license version required.

☐ CC-BY (for full details click here Creative Commons Attribution (CC BY) 4.0 International License)

☐ CC-BY-NC-ND (for full details click here Creative Commons Attribution Non Commercial No-derivatives (CC BY NC ND) 4.0 International License)

C. Please confirm that you have obtained permission from the original copyright holder. For ICE Publishing's copyright policy, please click here. ICE Publishing is a signatory to the STM Guidelines.

☑ I have obtained permission from the original copyright holder for the use of all subsidiary material included in this paper (E.g. for borrowed figures or tables).

Figure 2c

Click here to download Figures and line artwork Figure 2c.TIF

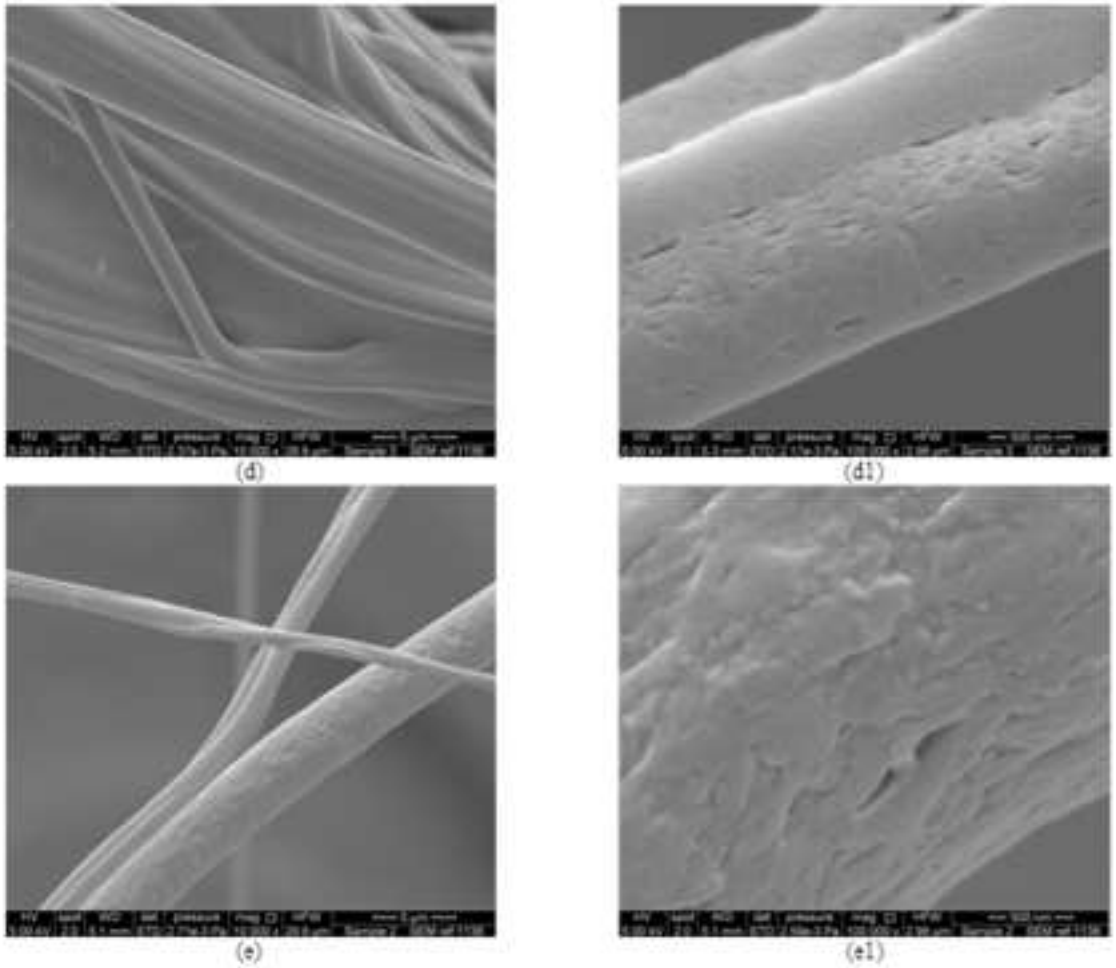

Figure 3a

Click here to download Figures and line artwork Figure 3a.TIF

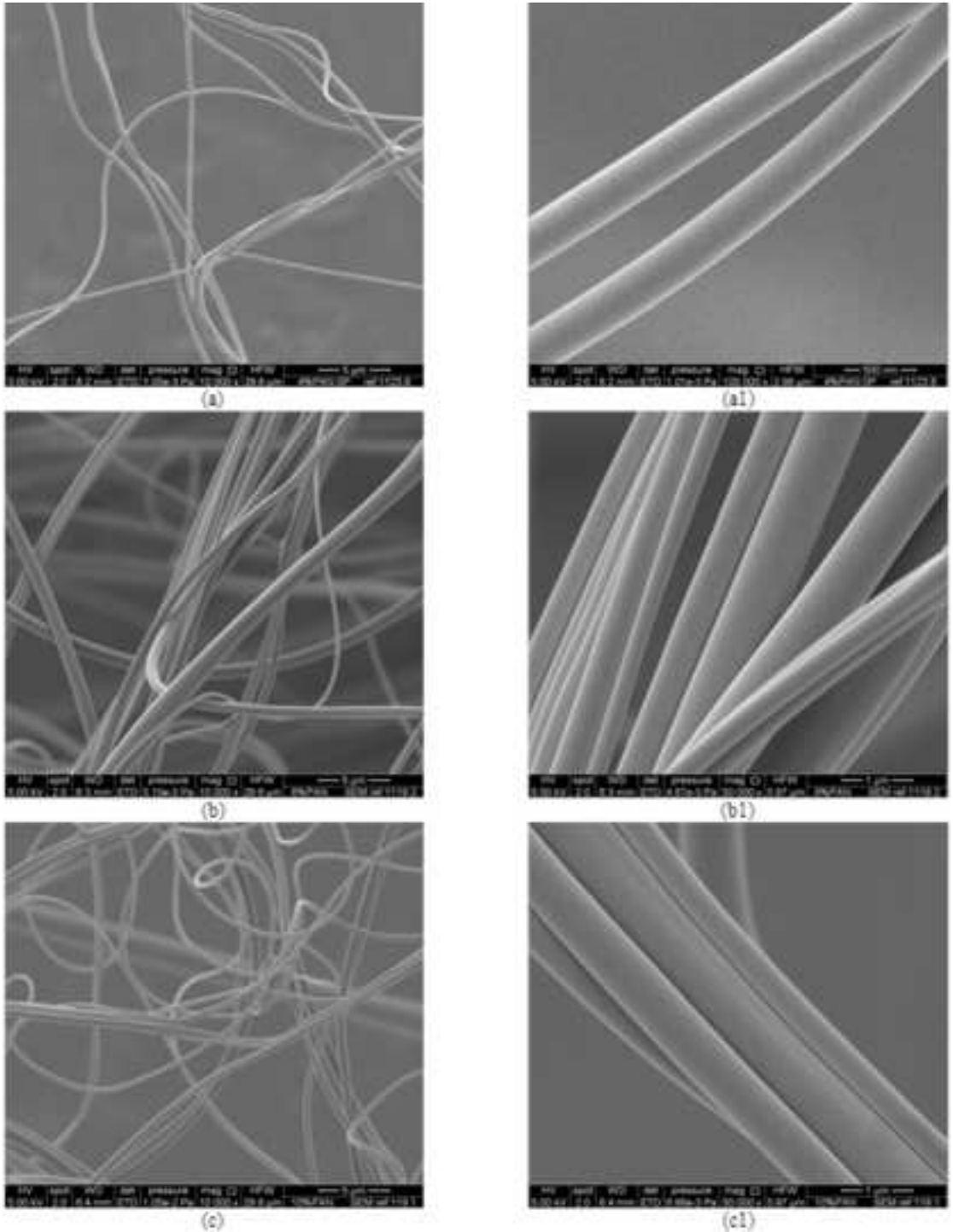

Figure 3b

Click here to download Figures and line artwork Figure 3b.TIF

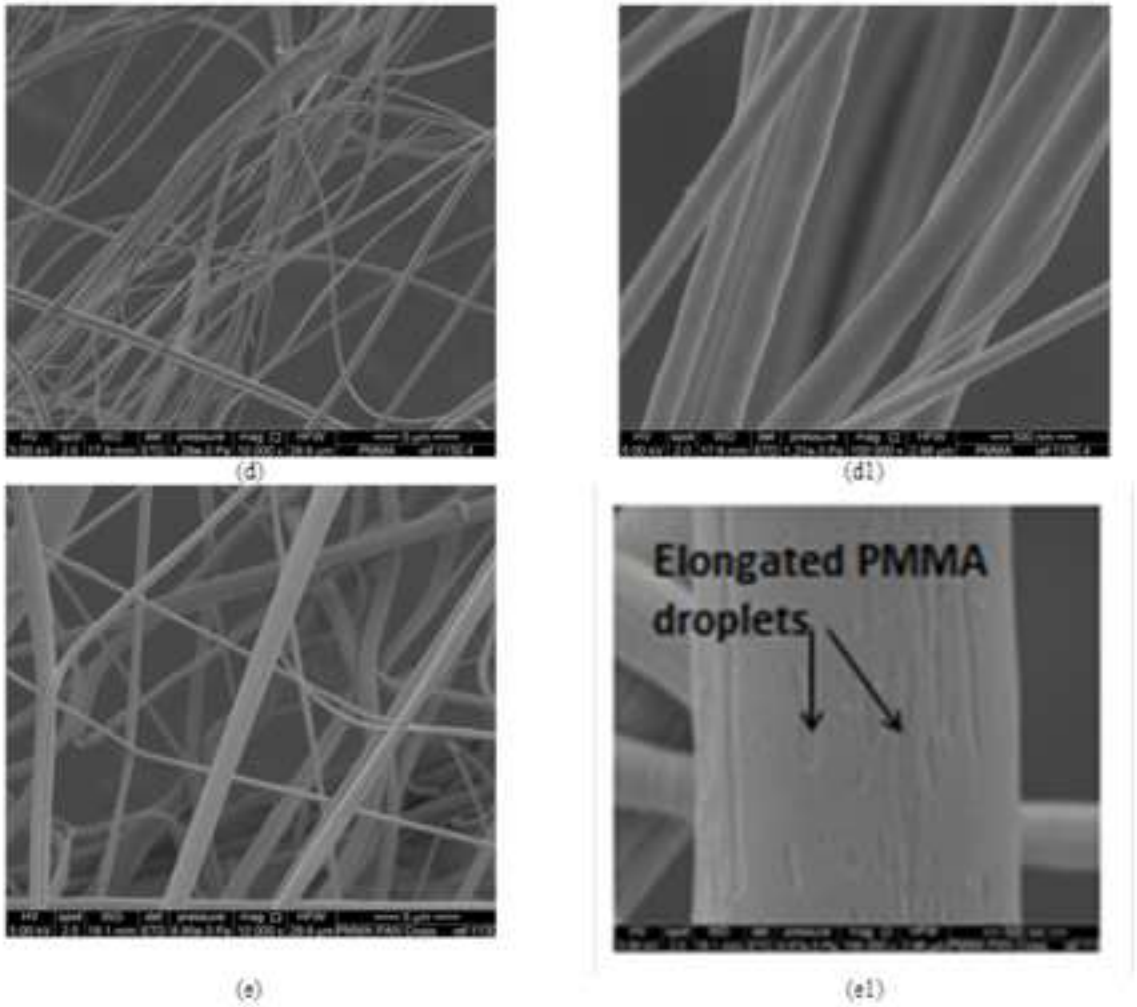

Figure 4

Click here to download Figures and line artwork Figure 4.TIF

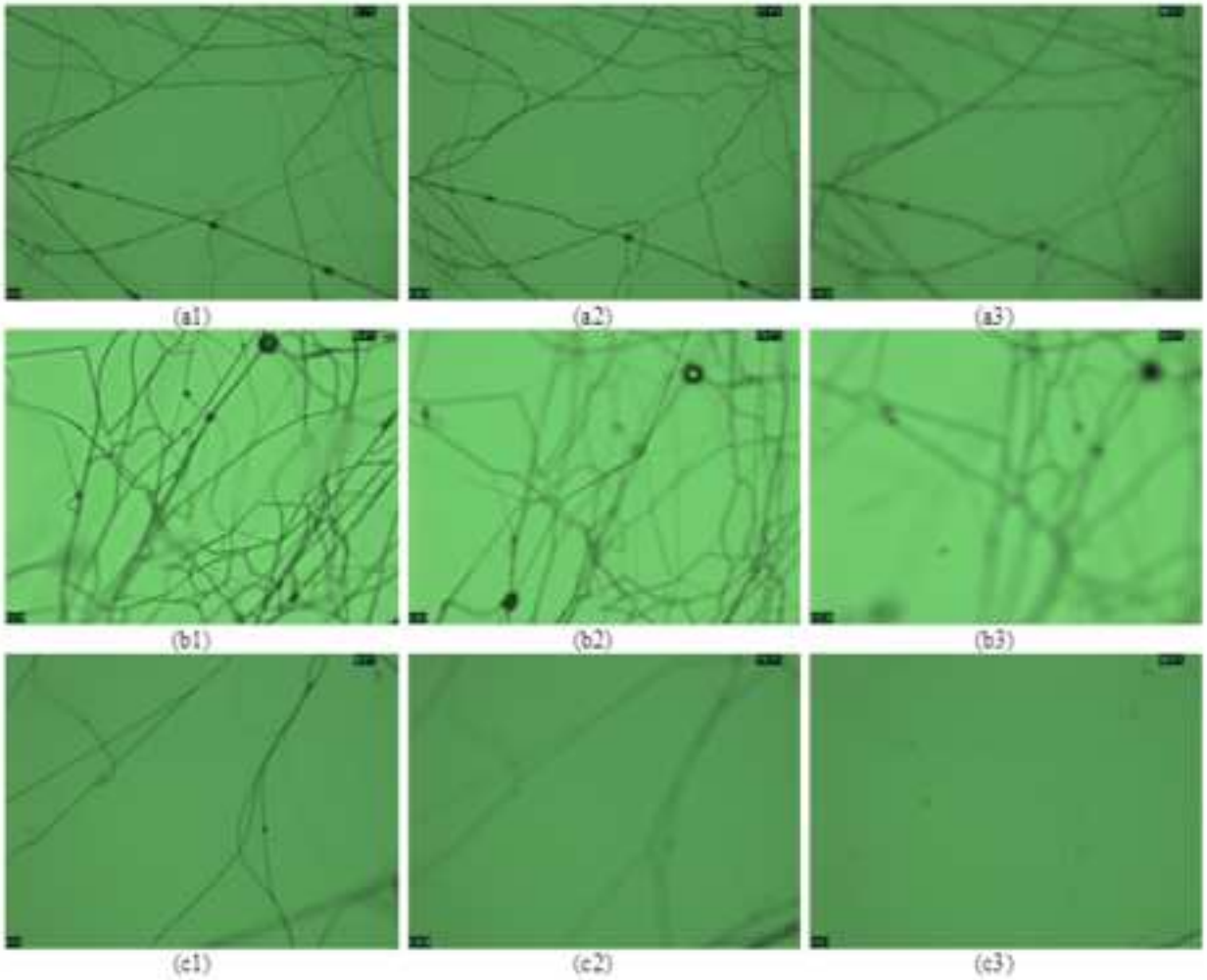

Figure 5

Click here to download Figures and line artwork Figure 5.tif

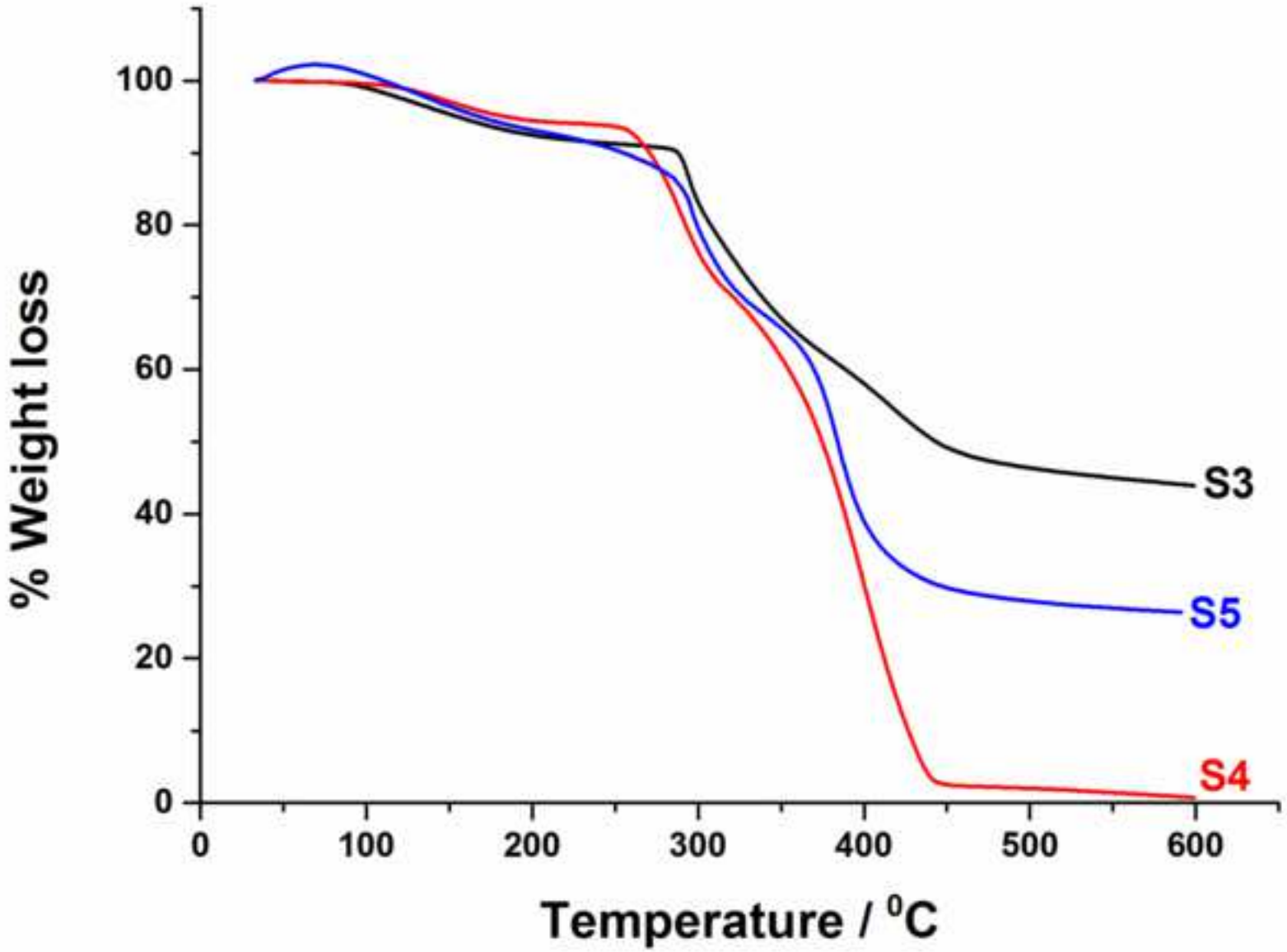

Figure 6

Click here to download Figures and line artwork Figure 6.TIF

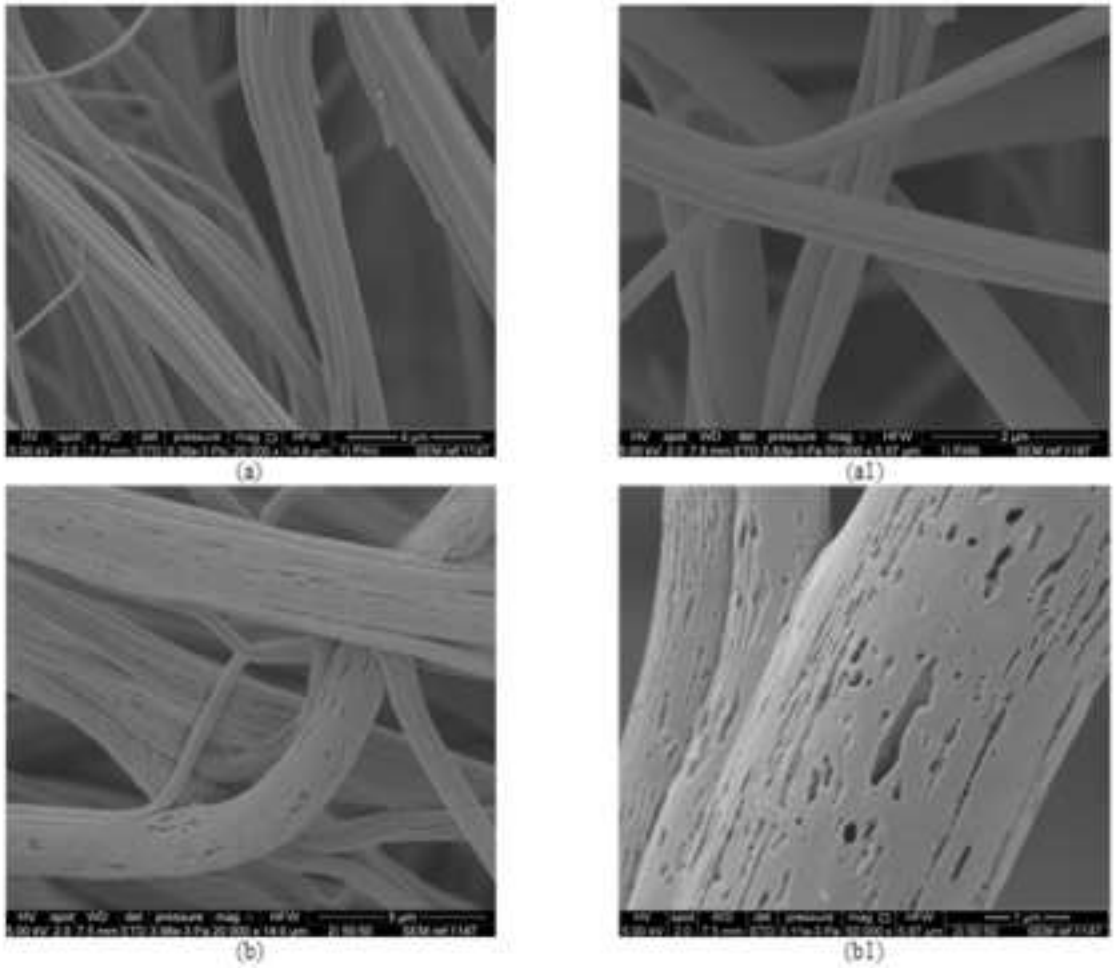

Table 1

Fiber sample	Fiber diameter (nm)
S1	410 ±130
S2	520 ±180
S3	450 ±150
S4	290 ±80
S5	580 ±260